universidade de aveiro
theoria poiesis praxis

Epigenetic responses of *Phaeodactylum tricornutum* to cadmium and ciprofloxacin exposure

Degree: Biology
Course Unit: Research Project
Sofia Valentim (112608)
Supervisors: Silja Frankenbach, Joana Santos
Academic Year: 2024/2025

dbio universidade de aveiro departamento de biologia

EPIBOOST

Funded by the European Union

This work was developed under the specific scope of the project EPIBOOST, funded by the European Union through the Grant 101078991 - views and opinions expressed are however those of the authors only and do not necessarily reflect those of the EU or the European Research Executive Agency; neither the EU or the granting authority can be held for them.

Index

Abstract

Pharmaceuticals and heavy metals are becoming more frequently detected in marine environments, but their impacts on primary producers are still poorly understood. This work assessed the physiological and genotoxic effects of the marine diatom Phaeodactylum tricornutum exposed to cadmium and ciprofloxacin (CIP) for 96 hours. Cultures were exposed to three concentrations of each contaminant EC10, EC20 and EC50, with increasing concentration, and effects were measured through maximum quantum yield (Fv/Fm), population growth (cell density), and DNA damage (comet assay).

Cadmium caused a temporary reduction in Fv/Fm and an increase in cell density at EC50, indicating recovery and hormesis. The DNA damage was concentration dependent but not statistically different. In contrast, CIP test showed moderate but lasting decline in Fv/Fm across all treatments, ciprofloxacin caused significant growth inhibition at EC20 and EC50, and an analysis to DNA damage exposed a biphasic genotoxic effect, with EC10 having substantially less damage than the other groups.

Results indicate contaminant-specific responses and endorse the application of P. tricornutum as a bioindicator. The integration of endpoints offers a sensitive system to evaluate physiological and genotoxic stress in marine ecotoxicology

Keywords: *Phaeodactylum tricornutum*; Cadmium; Ciprofloxacin; Photosynthetic efficiency; Genotoxicity.

1. Introduction

Diatoms are eukaryotic, unicellular, autotrophic and siliceous microalgae that play a fundamental role in marine ecosystems. They are responsible for about 40% of ocean and 20% of global primary production and play key roles in atmospheric carbon fixation to deep oceans via the biological carbon pump, a critical process for climate regulation (Buaya et al., 2019; Tréguer et al., 2018). They also produce approximately 20% of Earth's oxygen and are involved in nutrient recycling and represent an essential source of nutrition for most of marine life (Celi et al., 2022).

Diatom cells are enclosed in a frustule made of silicon dioxide (SiO_2) formed by two valves with species-specific morphological patterns (Smetacek, 1999). The rigid cell wall protects the cell and gives mechanical support for the formation of vacuoles (Pančić et al., 2019). Diatoms exhibit high adaptability due to their morphological and physiological plasticity, allowing them to thrive in environments subject to adverse changes, such as variations in temperature and pH (Fu et al., 2022).

Among diatoms, *Phaeodactylum tricornutum* is an unconventional diatom species as it has less silica compared to the majority of diatoms, and thus the cell wall is more flexible (Hendey et al., 1954; Russo et al., 2023). Due to this nature, it is able to exist in conditions of low silica concentration and possesses three morphotypes, which are fusiform, oval and triradiate (Borowitzka & Volcani, 1978; Song et al., 2020). Although such cellular plasticity is a sign of an ecological limitation, it facilitates growth and maintenance in artificial conditions. In this way, and considering that, as this species is highly susceptible to environmental disruption it is commonly used as a model organism in ecotoxicology (Russo et al., 2023).

Marine ecosystems are increasingly being threatened by anthropogenic contamination, particularly in coastal and estuarine areas where the concentration of contaminants is higher. Pharmaceuticals and heavy metals are contaminants of increasing concern. Cadmium, a non-essential metal, has been expanding its environmental occurrence as a result of industrialization and poor enforcement of environmental protection regulations. Concentrations higher than 25 mg/L can induce a series of physiological responses, from defense

mechanisms at the cellular level to growth inhibition and photobiological damaging effects in *Phaeodactylum tricornutum* diatoms (Han et al., 2020; Torres et al., 2000). Cadmium enters the cells via surface absorption and subsequently intracellular accumulation occurs over time (Ruangsomboon & Wongrat, 2006).

Pharmaceuticals, particularly antibiotics, have been employed extensively in medicine and animal husbandry, leading to their widespread presence in marine environments, which are the ultimate recipient of flowing contaminated waters (Hirsch et al., 1999). They are usually present in coastal waters at concentrations high enough to exert appreciable stress on organisms through bioaccumulation (Hagenbuch & Pinckney, 2012). Among them, ciprofloxacin is the most used fluoroquinolone antibiotic. It tackles multiple bacteria pathogenic diseases by inhibiting DNA replication and synthesis (Hooper, 2001). Notably, approximately 70% of administered antibiotics are discharged, via urine and feces, unchanged or partially digested into the environment, which promotes the increase of multidrug-resistant bacteria, induces physiological effects on organisms and then at the ecological level, ultimately modulating selection pressures within communities(Bhatt & Chatterjee, 2022; Massé et al., 2014). Consequently, most pharmaceuticals continue to persist in water even after treatment, especially because conventional water treatment plants are not efficient in ensuring the degradation of these compounds (Świacka et al., 2023). The frequent occurrence of xenobiotic contaminants in aquatic environments, including pharmaceuticals and heavy metals, along with their low biodegradation, is a significant environmental issue.

In order to assess the impact of cadmium and ciprofloxacin in the diatom *P. tricornutum*, exposures were carried out in this work, with the subsequent assessment of three phenotypic endpoints at different levels of biological organization: DNA damage, at the molecular level; photosynthetic efficiency, at the physiological level; cell yield, at the supra-individual level.

For assessing DNA damage, one widely used technique is the comet assay or single cell gel electrophoresis, originally described by Ostling & Johanson (1984) for detecting DNA damage in eukaryotic cells, more particularly single-strand breaks. The procedure consists in suspending and fixing cells in agarose onto microscope slides, after subjecting them to chemical lysis through detergent and

a high-salt solution to extract intracellular components. Subsequently, alkaline electrophoresis is performed to allow fragmented DNA to migrate, forming a shape resembling a comet (Olive & Banáth, 2006). The technique is well-accepted since it is simple, sensitive and can provide a quick evaluation, thus making it useful for environmental biomonitoring (Dhawan et al., 2008).

For assessing photosynthetic efficiency, a feasible tool is Pulse-Amplitude-Modulated (PAM) fluorometry, which analyzes in real time the functional state of Photosystem II (PSII) by measuring chlorophyll *a* fluorescence (Murchie & Lawson, 2013; Stock et al., 2019). Two parameters, Fo (minimum fluorescence) and Fm (maximum fluorescence), enable the calculation of the maximum photochemical efficiency of PSII as given by the quotient Fv/Fm = (Fm − Fo)/Fm. Theoretical values ranging from about 0.65 to 0.7 characterize healthy physiological condition in diatoms, while substantial reductions can be an indicator of stress or PSII damage (Gorbunov & Falkowski, 2021). The fluorescence yield of chlorophyll *a* is negatively correlated with photochemistry and heat dissipation: the higher the fluorescence, the less efficient these processes are. Photochemistry, in this context, refers to the use of absorbed light energy for electron transport in photosystem II (PSII), the first reaction of photosynthetic energy conversion. Therefore, healthier and more viable diatoms exhibit lower fluorescence values (Murchie & Lawson, 2013).

Given the importance of diatoms as key primary producers, it is important to characterize the hazardous potential that anthropogenic contaminants represent to these organisms, so that more robust information can be available to better understand the potential risks to the environment overall. In this sense, the primary objective of this study was to assess the physiological and genotoxic stress effects induced by cadmium and ciprofloxacin on the marine diatom *Phaeodactylum tricornutum*, a well-established model organism. These two pollutants, a metal and a pharmaceutical, were chosen to represent the two major classes of emerging contaminants found in the marine ecosystem. The growth, based on cell density yield, maximum photochemical efficiency of PSII (Fv/Fm), through PAM fluorometry, and DNA integrity, using the comet assay, where the endpoints used to tackle the objective.

2. Material & Methods

2.1. Maintenance of *Phaeodactylum tricornutum* cultures

Diatom cultures were maintained in artificial seawater medium prepared according to ISO 10253:2024 (International Organization for Standardization, 2024). The medium consisted of autoclaved artificial seawater made with filtered water and sea salt (Tropic Marin® Pro-Reef Sea Salt; 35 g/L), supplemented with 1 mL/L of nutrient solutions (K_3PO_4, $NaNO_3$, $Na_2SiO_3 \cdot 5H_2O$) and 0.5 mL/L of vitamins (thiamine hydrochloride, biotin, vitamin B_{12}) (International Organization for Standardization, 2024). Cultures were grown in 250 mL glass Erlenmeyer flasks containing 150 mL of the pre-prepared medium and 3 mL of 3-day-old inoculum from a mature culture. They were maintained in the laboratory at 21 ± 2 °C on an orbital shaker at 95 rpm, under artificial white light (140 µmol photon m^{-2} s^{-1}, 16L:8D photoperiod), and renewed every 4 days.

2.2. *Phaeodactylum tricornutum* exposure to cadmium and ciprofloxacin

Prior to exposure, the viability of the cultures was measured using Pulse amplitude modulated fluorometry by assessing the maximum quantum efficiency of the photosystem II, to ensure that only physiologically viable cultures were used. The methodology is described more precisely in the following subsection. The cultures were exposed to cadmium and ciprofloxacin for a total period of 96 hours. During that interval, the maximum quantum efficiency of PSII was recorded at the start (0 h) and after 96 hours to evaluate the effects of long-term contamination as well as to test the viability of the cultures.

Diatoms were exposed to three concentrations of each contaminant – Cadmium and ciprofloxacin - corresponding to the concentrations eliciting 10%, 20% and 50% cell yield inhibition, respectively EC10, EC20 and EC50 (Table 1), as estimated in previous work, plus a control treatment. Each treatment comprised three replicates.

Table 1- Concentration (mg/L) of cadmium and ciprofloxacin corresponding to each effective concentration.

	Concentration (mg/L)	
	Cadmium	Ciprofloxacin
EC10	0.099	0.114
EC20	0.293	0.202
EC50	1.856	0.533

Stock solutions for each contaminant were prepared by diluting Cadmium dichloride (CAS: 10108-64-2; Thermo Scientific Chemicals) or ciprofloxacin (CAS: 85721-33-1, Thermo Fisher Chemicals) in culture medium, achieving a final concentration of 12 mg/L and 80 mg/L, respectively.

The test solutions were prepared by combining the medium volume with the appropriate volume of stock solution to reach the desired contaminant concentrations of each treatment and then divided into three replicates. Then, a 3-day-old inoculum of *P. tricornutum* was added to each replicate, ensuring a target cell concentration of 10^4 cells/mL per replicate. The exposures were performed in the same conditions as the culture was maintained, except for the light, that was continuous, in accordance with ISO guideline 10253 (International Organization for Standardization, 2024). The exposure to cadmium was performed in 500 mL plastic Erlenmeyer flasks to avoid cadmium adsorption to glass containers (King et al., 1974), with a final test volume of 250 mL. Ciprofloxacin exposures were set up using 2-L glass Erlenmeyer flasks with 1 L of final test volume.

2.3. Pulse-Amplitude-Modulated fluorometry

Fv/Fm measurements were performed using Pulse-Amplitude-Modulated fluorometry (PAM) (Honeywill et al., 2002) with a PAM fluorometer (PamWin V3.22d) to assess viability and condition of the maintenance cultures.

This method is based on the fact that the absorbed light follows three paths: it is used for photochemistry, where electron transfer occurs in the reaction center of PSII, it is dissipated by heat or emitted as fluorescence (Baker, 2008); PAM fluorometry measures the fluorescence of chlorophyll *a*, specifically in the PSII.

This measurement occurs after the culture has been in absolute darkness for 15 min and is then exposed to an intense light pulse that causes light excitation (Schreiber, 2004). Two parameters were measured: Fo – minimum fluorescence that is measured after dark adaptation; and Fm - maximum fluorescence, measured after light saturation. With these results, the Fv/Fm was calculated, showing the maximum efficiency of PSII (Baker, 2008; Stock et al., 2019).

2.4. Population growth assessment via cell density

To estimate the diatom population growth, samples were collected and preserved at the beginning and end of both exposures by adding 20 µL of Lugol's iodine solution (Sigma-Aldrich) to 980 µL of culture.

Prior to counting, samples were diluted to reach a cellular concentration close to 10^6 cells per mL. After achieved, aliquots of 10 µL were placed in an improved Neubauer chamber (HIRSCHMANN EM Techcolor) with a micropipette. Cells were counted under a Leitz Laborlux S microscope, specifically the small squares within the four large corner quadrants, totaling 64 small squares. The number of cells was considered valid if reached at least 100 counts. If the number was lower, then dilution would be adjusted and the procedure repeated. The estimation was calculated using the formula:

$$Concentration = \frac{Number\ of\ cells\ x\ 10.000}{Number\ of\ square\ x\ dilution}.$$

2.5. Comet assay

Biomass collection and preparation

For each test replicate, 50 mL of test volume was initially collected from the Erlenmeyer flask and transferred to 50 mL Falcon tubes. The samples were centrifuged at 18 ×*g* for 5 minutes at room temperature (Eppendorf Centrifuge 5810R), and the supernatant was discarded. This procedure was repeated three additional times, resulting in four rounds of 50 ml, totaling up to 200 mL per replicate.

The resulting pellet was transferred to 2-mL Eppendorf tubes using micropipettes (tubes were filled so that they achieve similar weights) and subjected to further

centrifugation (Gyrozen 1524 for cadmium samples; VWR Micro Star 17R for ciprofloxacin samples) for 1-2 minutes at maximum speed. The pellet was washed with 2 mL of artificial seawater and centrifugated for 1.5 minutes at maximum speed (Gyrozen 1524), and the supernatant was discarded.

Silica Wall Dissolution and Nuclei Isolations

To access the genetic material, it is essential to dissolve the silica-based cell wall of the diatoms (Fu et al., 2022). The following protocol, adapted from Annunziata et al. (2021), was applied to the samples from the present work. After centrifugation (see above), the pellet was added with 400 µL of NH_4F (CAS: 12125-01-8; Sigma-Aldrich). The pellet was resuspended in this solution and incubated for 10 minutes at room temperature with periodic vortexing (Gyrozen 1524). Subsequently, 1.5 mL of filtered artificial sea water (Tropic Marin® Pro-Reef Sea; 35 g/L) was added, and the sample was vortexed again and centrifuged for 1 minute at maximum speed. The supernatant was discarded, and the pellet was washed once more with 2 mL of artificial seawater, followed by another centrifugation under the same conditions. After removing the supernatant, 200 µL of ice-cold Nuclear isolation buffer (NIB) was added to ensure that subsequent steps occur under optimal conditions for nuclear integrity (Annunziata et al., 2021). The microtubes were then kept on ice throughout the next steps. The samples were sonicated using an ultrasonic processor (Sonics Vibracell) through three cycles of 15 seconds at 60% intensity, with 10-second intervals. Finally, a further 100 µL of NIB was added to the sonicated samples, which were then filtered through a MCE Membrane 0.45 µm syringe filter (Millex - Merck Millipore)) into 1.5 mL microtubes.

DNA Damage Detection

DNA damage was assessed in the previously isolated cell nuclei. All protocol steps were performed under yellow light (≥ 540 nm), as its longer wavelength and lower photon energy minimize the risk of inducing additional DNA damage (de With & Greulich, 1995).

Solution Preparation

To perform the assay, ten different solutions were prepared:

- **Normal melting point agarose (1%)**
- **Low melting point agarose (0.5%)**
- **Lysis solution (stock)**
- **Final lysis solution**
- **Electrophoresis solution 1 (Na_2EDTA 200mM)**
- **Electrophoresis solution 2 (NaOH 10N = 10M)**
- **Electrophoresis buffer**
- **Neutralization buffer (Tris-HCl 0.4M)**
- **Staining solution (stock) – EtBr at 200 mg/mL**
- **Working staining solution – EtBr at 20 mg/mL**

To prepare 1% normal melting point agarose, 50 mL of 1x PBS (phosphate-buffered saline) was added to a beaker, and 0.5 g of agarose was dissolved. For the 0.5% low melting point agarose, 0.25 g of agarose was dissolved in 50 mL of 1x PBS. Both solutions were heated in a microwave until fully dissolved. Since evaporation can significantly alter solution volumes, after heating, the lost volume was replenished with 1x PBS.

The stock lysis solution was prepared for a final volume of 1000 mL by sequentially dissolving the following reagents in increasing order of quantity: 146.1 g of NaCl (2.5 M), 37.2 g of EDTA (100 mM), and 1.2 g of Tris-HCl (10 mM). After adding 700 mL of distilled water, the pH was adjusted to 10 with NaOH. The final volume was completed to 1000 mL with distilled water. This solution was stored in a container wrapped in aluminum foil to prevent light exposure and had a six-month shelf life.

The final lysis solution was prepared for a 200-mL volume (depending on the material size used) by mixing 2 mL of Triton X-100 and 20 mL of DMSO in the aluminum foil-wrapped lysis containers, completing the volume with the stock at 4°C and let sit for at least two hours.

For electrophoresis, solution 1 (Na_2EDTA 200 mM) was prepared by dissolving 14.89 g of Na_2EDTA in 200 mL of distilled water, adjusting the pH to 10 with NaOH. This solution was stored at room temperature. Solution 2 (NaOH 10N = 10M) was prepared by dissolving 200 g of NaOH in 500 mL of distilled water, also stored at room temperature. The electrophoresis buffer was obtained by mixing

5 mL of solution 1 with 30 mL of solution 2 and adding distilled water at 4°C to a final volume of 1000 mL. The electrophoresis system operated at a voltage of 0.7 V/cm.

The neutralization buffer (Tris-HCl 0.4 M) was prepared by dissolving 48.5 g of Tris in 700 mL of distilled water, adjusting the pH to 7.5 with HCl, and completing the volume to 1000 mL. After preparation, the solution was kept at 4°C and stored at room temperature before use.

The stock staining solution (EtBr at 200 mg/mL) was prepared by dissolving 10 g of ethidium bromide in 50 mL of distilled water. The working staining solution (EtBr at 20 mg/mL) was obtained by a 1:10 dilution (1 mL of the stock solution in 9 mL of distilled water). To prevent light exposure, both solutions were stored in light-protected containers wrapped in aluminum foil.

Procedure

With the solutions prepared, the Comet assay protocol was initiated.

First, microscope slides were prepared. To ensure adhesion of the low melting point agarose, 600 µL of 1% normal melting point agarose was first deposited onto the slides, covered with a coverslip. After solidification, the coverslip was removed, and the slides were left to dry for at least one day.

To suspend cells and isolated nuclei on the slides and allow cell lysis, 20 µL of the cell suspension was added to the previously prepared 0.5% low melting point agarose. The mixture was applied to the slide using a micropipette. After solidification, the coverslips were removed, the slides were immersed in a histological staining box containing the lysis solution and stored at 4°C for at least one hour. After lysis, the slides were transferred to the electrophoresis tank, positioned with the identification facing the negative pole. DNA denaturation occurred before electrophoresis when the slides were placed in the electrophoresis buffer for 15 minutes. Then, a current of 300 mA was applied for 10 minutes.

After electrophoresis, the slides were removed from the tank and immersed in a neutralization buffer (Tris-HCl 0.4 M). In the first wash, the solution was

completely removed, while in the following two washes, the slides remained submerged for five minutes each. Subsequently, they were washed with ethanol and left to air-dry.

For DNA staining, 80 µL of ethidium bromide solution was applied to the slides, covered with a coverslip. The slides were stored and protected from light with aluminum foil. After two days, they were sealed with nail polish and stored again under light protection.

Slides were kept refrigerated for up to three weeks before visualization.

Visualization and Nuclei Counting

Samples were analyzed using a Confocal Zeiss LSM880 Airyscan confocal microscope equipped with a Plan-Apochromat 100×/1.40 Oil DIC objective. Imaging was performed using an Alexa Fluor 568 fluorophore, with excitation provided by a DPSS 561-10 laser and a 405-30 diode. Signal detection was optimized using an MBS 488/561 beam splitter. Data acquisition was conducted on an AxioObserver platform in LSMCOLLI_V mode. Nuclei counting was performed manually, with a minimum of 100 nuclei/comets per sample. The classification of nuclei was divided into two categories:

1. **Damaged** – nuclei with reduced brightness or a surrounding halo.
2. **Undamaged** – nuclei with intense brightness and no halo.

2.6. Statistical Analysis

The maximum quantum efficiency of PSII (Fv/Fm), cell density, and the percentage of damaged nuclei were the dependent variable used to compare the different treatments exposed to cadmium and ciprofloxacin. Before performing the parametric tests, normality of data distribution and homogeneity of variance were verified using the Shapiro–Wilk test and the Brown–Forsyth test, respectively. After confirming the conditions, a two-way analysis of variance (ANOVA) was carried out to determine if there were statistically significant differences between the treatment groups. In the cases where the ANOVA denoted a significant effect of the stressor across treatments (p value <0.05),

pairwise comparisons were performed using the Holm–Šidák method for a more specific analysis between groups, or the Dunnet test for a specific comparison versus the control group.

3. Results

Figure 1 regards the exposure to cadmium; initial values ranged from 0.66 to 0.42. By the end of the experiment, a recovery was recorded in all the concentrations, and Fv/Fm reached levels comparable to the control group.

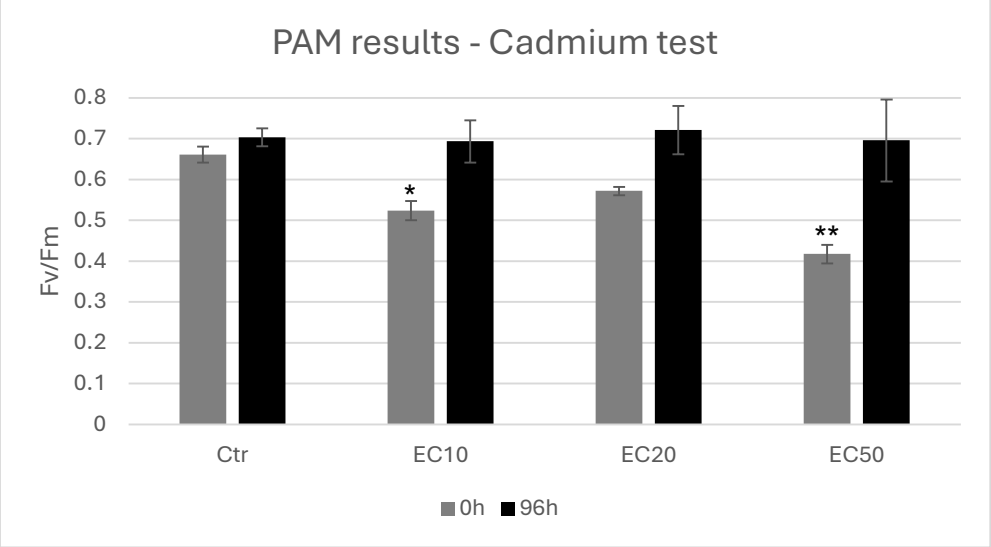

Figure 1- Maximum quantum efficiency of PSII (Fv/Fm) measured in the beginning (0h) and in the end (96h) of the cadmium test exposure period. The results compare different groups – the control group (Ctr) without contaminant and the treatment groups (EC10, EC20 and EC50), corresponding to increasing cadmium concentrations. The bars represent the mean values of the replicates, while the error bars show the standard deviation of the measurements. Asterisks indicate statistically significant differences compared to the control group (Ctr): $p < 0.05$ (*), $p < 0.01$ (**); based on ANOVA followed by Dunnett's post hoc test.

Parametric test assumptions were fulfilled: the data passed the Shapiro–Wilk test for normality ($p = 0.974$) and the Brown–Forsythe test for equal variances ($p = 0.334$). Analysis detected a significant interaction between treatment and time ($F_{(3,8)} = 4.851$; $p = 0.033$), indicating distinct effects induced by the treatment, depending to the period of exposure. At 0 hours, Dunnett's post-hoc test showed that Fv/Fm was significantly decreased in both the EC10 ($p = 0.008$) and EC50 ($p < 0.001$) treatments compared to control, while the EC20 treatment was not

statistically different (p = 0.093). However, after 96 hours of exposure, no significant differences were observed between any treatment and the control, since all p-value were greater than 0.9), suggesting a recovery of photophysiological performance in all cadmium concentrations.

Figure 2 indicates that the Fv/Fm values for the test with ciprofloxacin remained relatively stable throughout the 96-hour ciprofloxacin exposure period. Initial reading ranged between 0.69 and 0.72, decreasing slightly to values between 0.63 and 0.68 by the end. This reflects a general but modest decline across all treatments, with the most noticeable reductions, though still mild, occurring in EC20 and EC50.

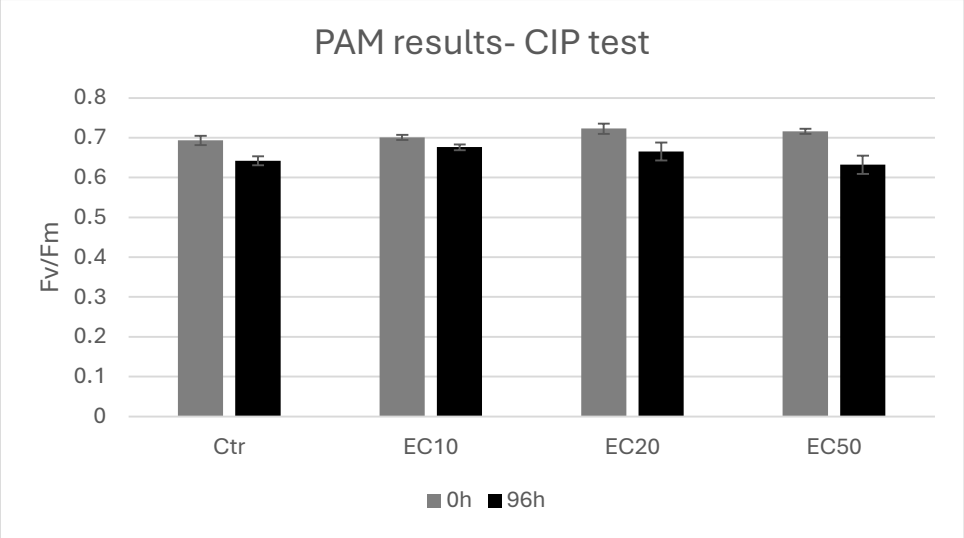

Figure 2- Maximum quantum efficiency of PSII (Fv/Fm) measured at the beginning (0 h) and the end (96 h) of the ciprofloxacin test exposure period. The results compare different groups – the control group (Ctr) without contaminant and the treatment groups (EC10, EC20 and EC50), corresponding to increasing ciprofloxacin concentrations. The bars represent the mean values of the replicates, while the error bars show the standard deviation of the measurements.

For ciprofloxacin, the Shapiro–Wilk test indicated a significant deviation from normality (p < 0.050), but the Brown–Forsythe test confirmed the equality of variances (p = 1.000). Given the robustness of repeated measures ANOVA the analysis was performed. It revealed no significant interaction between treatment and time ($F_{(}3,8_{)}$ = 0.011; p = 0.998), meaning no statistical differences among treatment groups at either time point. In contrast, there was a significant effect of time ($F_{(}1,8_{)}$ = 15.944; p = 0.004), due to an overall increase in Fv/Fm from 0 h to

96 h. Despite this, the increase was consistent across all treatments and not due to specific responses to ciprofloxacin.

Figure 3 shows the cell density in each treatment of the exposure to cadmium, it was measured two times, clearly showing growth over time. At the beginning of the test, values remained around 1.05 × 10^6 cells/mL, as planned. After 96 hours, a marked increase was observed across all treatments, with the EC50 group showing the highest cell concentration.

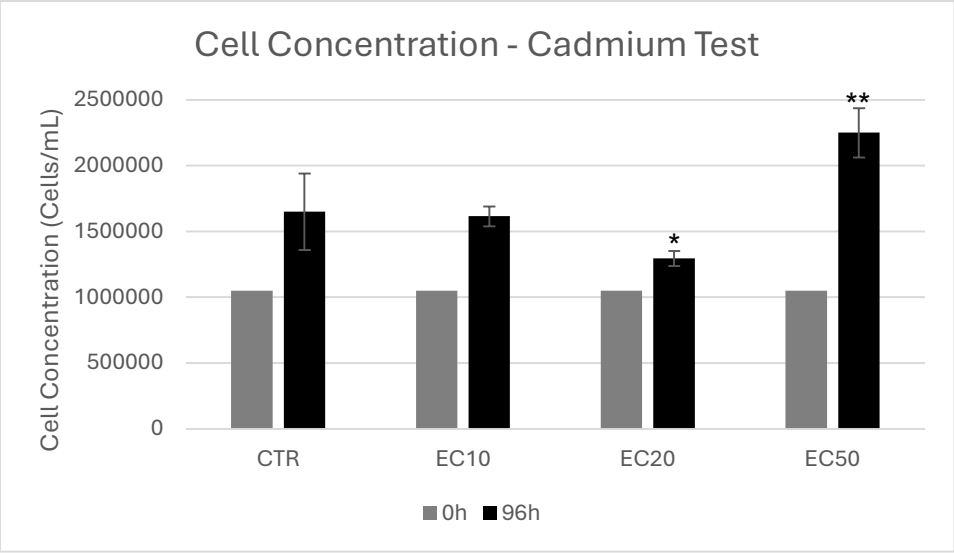

Figure 3- Cell density measured at the beginning (0 h) and the end (96 h) of the ciprofloxacin test exposure period. The results compare different groups – the control group (Ctr) without contaminant and the treatment groups (EC10, EC20 and EC50), corresponding to increasing ciprofloxacin concentrations. The bars represent the mean values of the replicates, while the error bars show the standard deviation of the measurements. Asterisks indicate statistically significant differences compared to the control group (Ctr): $p < 0.05$ (*), $p < 0.01$ (**); based on ANOVA followed by Dunnett's post hoc test.

The Shapiro–Wilk test verified normality ($p = 0.146$), though the Brown–Forsythe test did not ($p < 0.050$), suggesting heterogeneity of variances. Despite that, two-way repeated measures ANOVA was performed. It was detected a significant interaction between treatment and time ($F_{(}3,8_{)} = 16.907$; $p < 0.001$). At 96 h, significant differences were observed, when compared with the control: EC20 ($p = 0.007$) and EC50 ($p < 0.001$), EC20 treatment resulted in a much lower density, while EC50 substantially higher. No significant difference was found with EC10 ($p = 0.995$).

Figure 4 demonstrates the cell concentration (cells/mL) calculated at the starting point and after 96 hours exposure to ciprofloxacin. Starting cell concentration was similar in all groups and was around 1.05 × 10^6 cells/mL. After exposure to the antibiotic for 96 hours, there was increased cell concentration across all treatments but with larger growth where lower concentration of the antibiotic was used. The control group had the highest final cell density, and the EC50 group had the least increase.

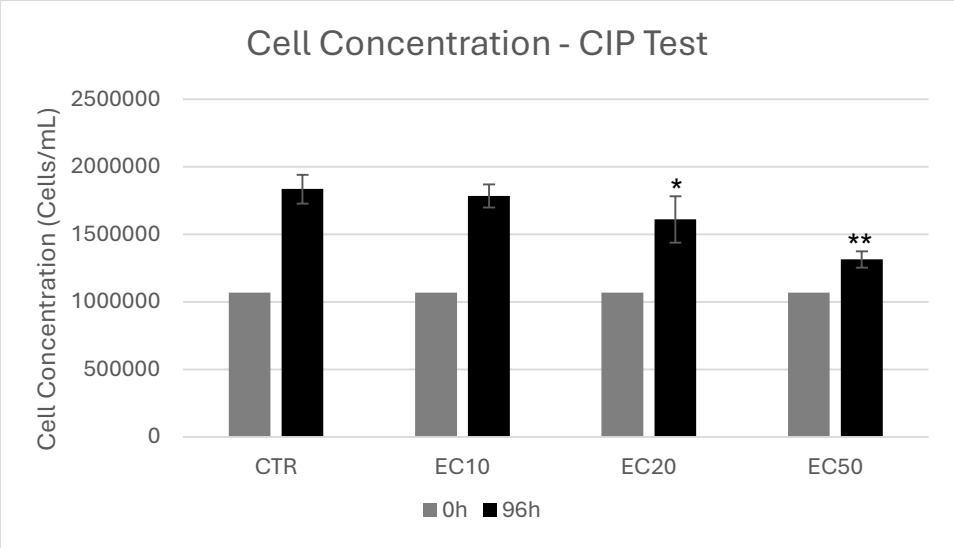

Figure 4- Cell concentration (cells/mL) measured at the beginning (0 h) and the end (96 h) of the ciprofloxacin test exposure period. The results compare different groups – the control group (Ctr) without contaminant and the treatment groups (EC10, EC20 and EC50), corresponding to increasing ciprofloxacin concentrations. The bars represent the mean values of the replicates. Asterisks indicate statistically significant differences compared to the control group (Ctr): $p < 0.05$ (*), $p < 0.01$ (**); based on ANOVA followed by Dunnett's post hoc test.

Parametric test assumptions were fulfilled (Shapiro–Wilk: p = 0.994 and Brown–Forsythe: p = 0.098). In parallel with the cadmium results, exposure to ciprofloxacin lead to a statistically significant interactions between treatment and time ($F_(3,8)$ = 11.733; p = 0.003). Equally, at 96h, EC20 (p = 0.035) and EC50 (p < 0.001) showed significant differences exhibiting considerably less cell density relative to the control, while EC10 was not significantly different (p = 0.789).

The results for the comets are presented through two graphical representations for each contaminant (Figures 5-8), highlighting both absolute and proportional changes.

Figure 5 illustrates the absolute number of nuclei categorized as either damaged or undamaged in each experimental condition: Control (CTR), EC10, EC20 and EC50. In the control group (CTR), the numbers of damaged and undamaged nuclei are relatively close, both ranging between 60 to 70 nuclei. At EC10, there is an increase in the number of damaged nuclei, while the number of undamaged nuclei decreases slightly. EC20 shows a more pronounced rise in the damaged nuclei, reaching approximately 140, while undamaged nuclei also increased slightly. At EC50, the number of damaged nuclei remains high and slightly increases compared to EC20, whereas the number of undamaged nuclei decreases again.

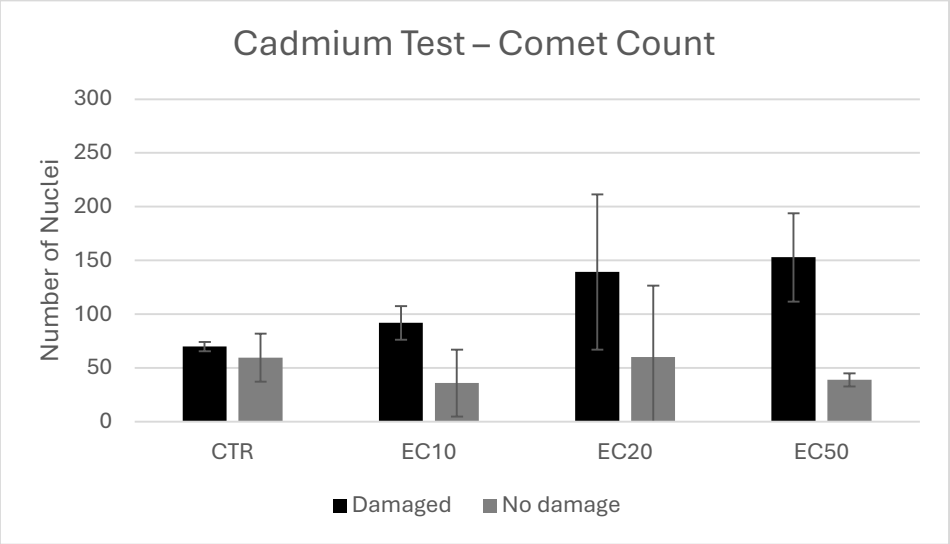

Figure 5- Absolute number of nuclei (damaged and undamaged) measured during the cadmium test. The results compare the control group (CTR) with cadmium-contaminated groups (EC10, EC20, EC50), corresponding to increasing cadmium concentrations. Black bars represent the counted number of damaged nuclei, while gray bars represent counted undamaged nuclei. Bars indicate the mean values of the replicates, and the error bars represent the standard deviation.

Figure 6 presents the relative proportion of damaged and undamaged nuclei expressed as percentages. In the control group, damaged nuclei represented approximately 55%, while undamaged nuclei accounted for around 45%, indicating a balanced control condition. Upon exposure to EC10, the proportion of damaged nuclei increased to roughly 72%, while undamaged nuclei decreased to 28%. The EC20 group showed a similar distribution, with damaged nuclei constituting around 70% of the total. In the EC50 condition, the percentage of

damaged nuclei further increased to approximately 80%, while undamaged nuclei fell below 20%.

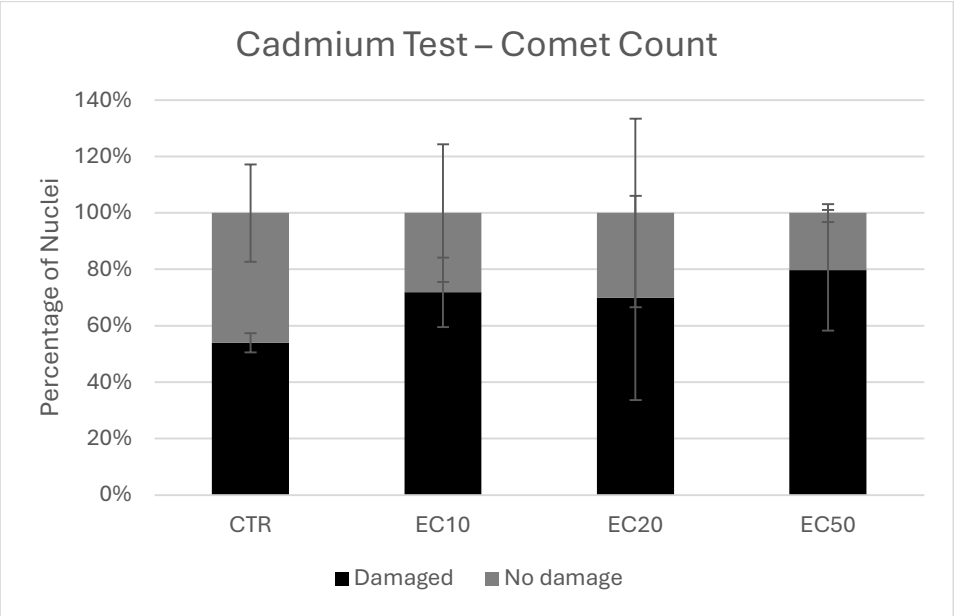

Figure 6- Stacked bar chart showing the percentage of damaged and undamaged nuclei measured after performing the comet assay, which was conducted following the cadmium test. The results compare different groups – the control group (Ctr) without contaminant and the treatment groups (EC10, EC20 and EC50), corresponding to increasing cadmium concentrations. Black bars represent the percentage of damaged nuclei, while gray bars represent percentage undamaged nuclei. Bars indicate the mean values of the replicates, and the error bars represent the standard deviation.

The one-way ANOVA was used to assess whether statistically significant differences existed among the percentage of damaged nuclei between the cadmium exposure groups (control (CTR), EC10, EC20, EC50).

The data passed the requirements for parametric analysis: the Shapiro–Wilk test confirmed the normal distribution ($p = 0.862$), and the Brown–Forsythe test verified the homogeneity of variances ($p = 0.210$), thus justifying the use of ANOVA.

The mean percentage of damaged nuclei increased with the increasing cadmium concentrations, ranging from 55.02% in the control group to 79.11% in the EC50 group. However, the ANOVA results did not detect statistically significant results ($F_{3,\ 8} = 3{,}29$; $p = 0.079$), and therefore, the observed trend could not be established at the significance level $\alpha = 0.05$.

Statistical power of the test was calculated at 0.384, below the recommended threshold of 0.800. This finding suggests that there was only a probability of 38.4% identifying an existing difference.

Figure 7 displays the absolute number of damaged and undamaged nuclei for each condition tested. In the CTR group, a high number of damaged nuclei is observed, accompanied by a relatively low count of undamaged nuclei. Upon exposure to EC10, a reduction in the number of damaged nuclei is detected, while the number of undamaged nuclei increases significantly. At EC20, a sharp increase in the number of damaged nuclei is evident, with undamaged nuclei becoming low. At the highest concentration, EC50, only damaged nuclei are observed, although the number of damaged nuclei slightly decreases compared to EC20.

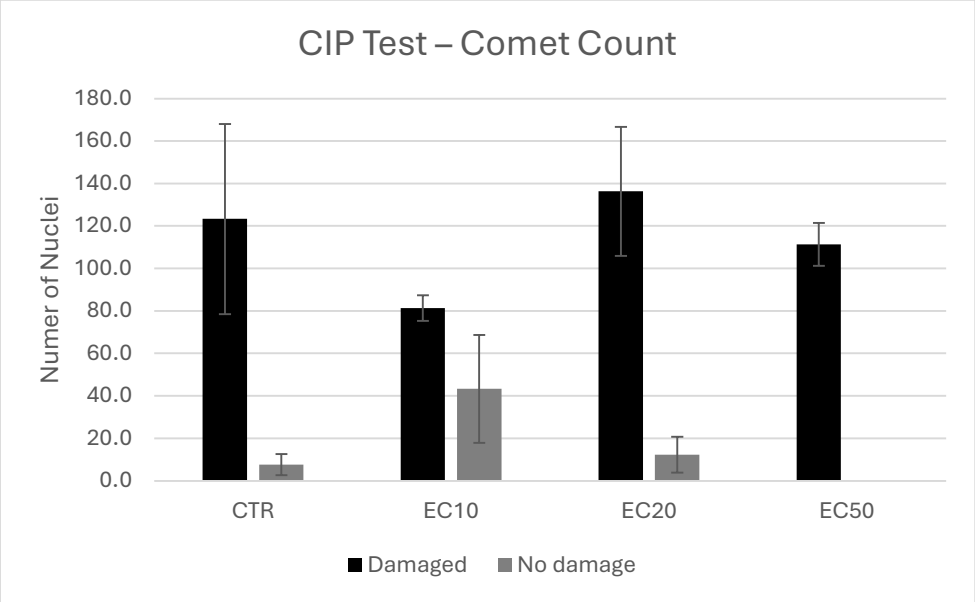

Figure 7- Absolute number of nuclei (damaged and undamaged) counted after performing the comet assay, which was conducted following the ciprofloxacin test. The results compare different groups – the control group (Ctr) without contaminant and the treatment groups (EC10, EC20 and EC50), corresponding to increasing ciprofloxacin concentrations. Black bars represent the counted number of damaged nuclei, while gray bars represent counted undamaged nuclei. Bars indicate the mean values of the replicates, and the error bars represent the standard deviation.

Figure 8 displays the percentage of nuclei classified as damaged or undamaged in each condition. In the CTR group, over 90% of nuclei are damaged. EC10 demonstrates the lowest level of DNA damage, with approximately 66% of nuclei

damaged and 34% undamaged. EC20 shows an increase in the percentage of damaged nuclei to around 95%, while undamaged nuclei represent only a minimal fraction. At EC50, 100% of the nuclei are identified as damaged, indicating complete nuclear damage at the highest concentration tested.

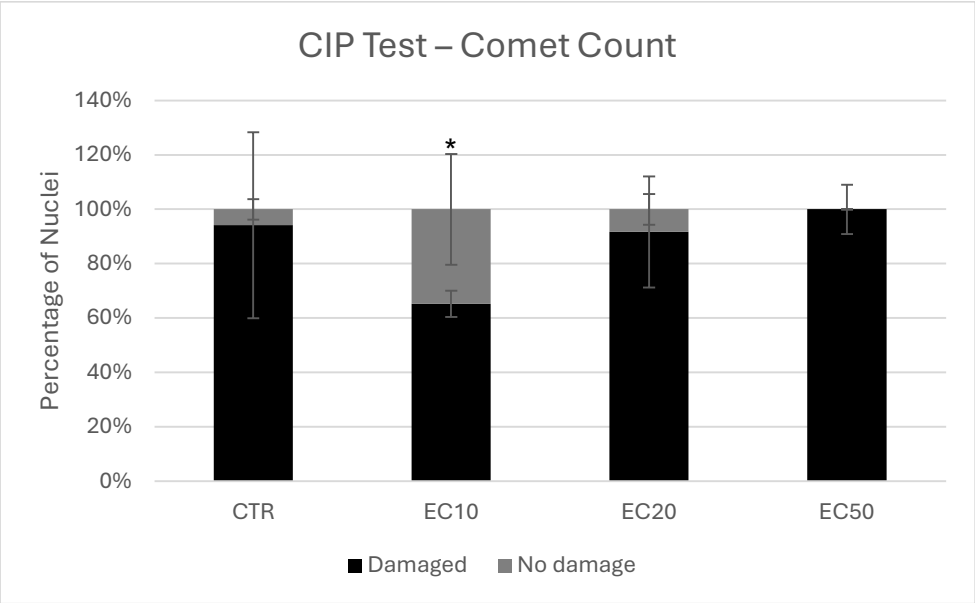

Figure 8- Stacked bar chart showing the percentage of damaged and undamaged nuclei measured after performing the comet assay, which was conducted following the ciprofloxacin test. The results compare different groups – the control group (Ctr) without contaminant and the treatment groups (EC10, EC20 and EC50), corresponding to increasing ciprofloxacin concentrations. The stacked columns represent the proportion of damaged nuclei (black) and undamaged nuclei (gray) within the total nuclei counted. Bars indicate the mean values of the replicates, and the error bars represent the standard deviation. Asterisks indicate statistically significant differences compared to the control group (Ctr): $p < 0.05$ (*), $p < 0.01$ (**); based on ANOVA followed by Holm–Šidák post hoc test.

The ANOVA was also used to analyze differences in the percentage of damaged nuclei among ciprofloxacin treatment groups. The data fulfilled the conditions for parametric analysis: the Shapiro–Wilk test indicated normality ($p = 0.099$), and the Brown–Forsythe test indicated homogeneity of variances ($p = 0.264$)

ANOVA revealed a statistically significant impact on DNA damage ($F_{3, 8} = 10{,}93$; $p= 0.003$). The test power was 0.956, and for this reason it is sensitive to detect true differences.

Post-hoc tests were conducted according to Holm–Šidák method, indicating that there were significant differences between the EC10 and all other treatment groups: EC50 ($p = 0.004$), CTR ($p = 0.012$) and EC20 ($p = 0.015$). However, no significant differences were observed between the EC50 and EC20 groups ($p =$

0.558), the EC50 and the control group (p = 0.597), or the control and EC20 groups (p = 0.761).

4. Discussion

The findings of the research revealed the sensitivity of *P. tricornutum* to cadmium and ciprofloxacin with different response patterns, physiological and genotoxic.

4.1. Photophysiological responses to cadmium and ciprofloxacin

The PAM fluorometry assays showed variable effects of these contaminants on the efficiency of PSII. When exposed to cadmium, a significant decrease in Fv/Fm was initially observed in EC10 and EC50 relative to the control. Which subsequently recovered after 96 hours, reaching levels statistically indistinguishable from the control. The recovery pattern is in agreement with previous observations in *P. tricornutum* made by Brembu et al., (2011), who noted that this species showed high tolerance to cadmium concentrations up to 123 µg/L with no effect on chlorophyll and growth, only minor transcriptional changes. Diatoms' ability to recover photosynthetic efficiency under metal stress has been attributed to several cellular defense mechanisms that include the induction of antioxidant systems and the synthesis of metal-binding compounds, such as phytochelatins (Branco et al., 2010; Gorbunov & Falkowski, 2021).

During the ciprofloxacin test a mild decrease in Fv/Fm was identified by 96 hour period, initially from 0.69-0.72 to 0.63-0.68. This decline was consistent across all the treatments, and no statistically significant differences were found between them, however, a significant effect of time was observed. Despite the lack of significant variation between groups, the pattern could suggest that P. tricornutum has a high photosynthetic capacity under antibiotic stress. The relatively stable Fv/Fm and inability to recover over time suggest little to none PSII damage at the ciprofloxacin concentrations tested, *P. tricornutum* culture maintained close to normal photosynthesis over the 96 hours. Nerveless, the absence of recovery is consistent with the ability of fluoroquinolone antibiotics to inhibit PSII electron transport impairing photosynthesis (Aristilde et al., 2010).

4.2. Growth patterns under contaminant stress

Cell density measurements support the photosynthetic findings. Statistical analysis confirmed that cadmium exposure caused significant interaction between treatment and time. At 96h, the treatments EC20 and EC50 also showed significant statistical differences. The unexpected rise noted at the highest cadmium treatment (EC50) may be explained by hormetic compensation, inducing cellular defense mechanisms, such as, increasing cell replication or activating antioxidant enzymes pathways to neutralize reactive oxygen species (ROS) produced under cadmium stress (Branco et al., 2010; Gorbunov & Falkowski, 2021). For, ciprofloxacin, a similar interaction was detected, with significant decreases in EC20 and EC50 when comparing with the control. The results confirm concentration dependent growth inhibition, most likely due to the ciprofloxacin binding to DNA gyrase and topoisomerase IV, disrupting DNA replication (Hooper, 2001).

It is important to note that the culture used was not axenic, meaning it contained not only *P. tricornutum*, but also other associated microorganisms. Consequently, the effects observed may not solely be the result from direct toxicity to the diatom, but also from the impact on the surrounding microorganisms that collectively form the holobiont. Ciprofloxacin is used to target various prokaryotic cells, like bacteria, and can reduce its overall population in the culture, which can negatively affect the ecological interactions within the holobiont (Amin et al., 2012). As highlighted by Moejes et al. (2017), *P. tricornutum* usually coexists with various dynamic bacterial families that interact metabolically by nutrient cycling, metabolite exchange, and contribute to the stability of the culture. Thus, they play a critical role in supporting growth and stress tolerance, and disturbance of the microbiota is likely to heavily influence the physiological responses of the diatom.

4.3. Genotoxic effects showed by the comet assay

The comet assay revealed dose-dependent genotoxicity. The cadmium exposure resulted in a rising proportion of damaged nuclei (from ≅55% in controls to ≅79% at EC50). Despite the concentration dependent trend, statistical differences

weren't found, potentially due to the low test power. Although cadmium is capable of causing DNA damage both directly, by binding to DNA repair enzymes, and indirectly, via ROS (Han et al., 2020). The finding suggests that cadmium can cause genotoxic stress at higher concentrations of cadmium, though the short term of exposure or high repair potential prevented significance.

In contrast, ciprofloxacin exposure data revealed a more complex genotoxic pattern. ANOVA revealed a significant effect by the treatments. The control group had high levels of DNA damage, suggesting some procedural stress or intrinsic culture conditions. Notably, the lowest ciprofloxacin concentration (EC10) caused significantly lower level of damage, while both EC20 and EC50 had very high levels of damage, making them not differ significantly from the control, supposedly on account to the elevated damage in the control. The low damaged observed in EC10 could represent a biphasic effect: low doses of antibiotic (EC10) could have triggered DNA repair mechanisms or slowed cell cycle, reducing apparent damage, whereas higher doses (EC20–50) overwhelmed repair mechanisms, demonstrating a threshold effect. Fluoroquinolones are known to intercalate DNA and inhibit topoisomerases, causing DNA breaks and oxidative damage (Dhawan et al., 2008; Olive & Banáth, 2006) as indicated by the number of comets at higher concentrations of ciprofloxacin.

4.4. Biomonitoring and ecological implications

Diatoms have been recognized as sensitive sentinels of environmental pollution based on their rapid response to contaminants and their fundamental role in marine food webs (Russo et al., 2023). With that in mind, the sensitivity of *P. tricornutum* to both heavy metals and pharmaceuticals points to the promising use of this species as a bioindicator, with specific endpoints, for example, the photophysical responses (Fv/Fm) for assessing the combined impacts of emerging pollutants.

The persistence of pharmaceutical compounds in marine systems, along with bioaccumulation, generates long lasting ecological threats. Climate change can also alter contaminant transport and bioavailability, which may alter the exposure

routes and impacts observed under controlled laboratory settings (Kholssi et al., 2023).

The capacity of the comet assay to identify DNA damage at concentrations that are environmentally relevant qualifies genotoxicity as a useful biomarker for early warning systems when monitoring marine pollution.

4.5. Methodological considerations

This work has limitations, and a few methodological points warrant discussion. The nuclear isolation technique involving the use of NH_4F to dissolve the silica frustule was key to the recovery of DNA from diatom, however, this procedure may lead to introduction of artifacts or partial cell lysis. These are partially compensated by the strict application of the same methods in all treatments, including the control, but natural variations while executing the protocol should not be fully disregarded. Besides this, the discrimination of nuclei into damaged and undamaged is difficult due to the small size of the nuclei, which made it impossible to qualify the damage in a broad range and lead to an oversimplification of the gradient of DNA damage, possibly failing to discriminate subtle variations in the degree of damage. The outcomes of the comet assay were indeed very variable and, unexpectedly, there was high damage in controls, it is conceivable that this reflects methodological stress or would be minimized by having more replicates to improve statistical power. Only two biomarkers (genotoxicity and photosynthetic efficiency) were used; other endpoints (antioxidant enzyme activity, membrane integrity, cell-cycle markers) could be more revealing.

5. Conclusion

This research effectively demonstrated the advantages of integrating PAM fluorometry and comet assay techniques in determining the ecotoxicological impacts of cadmium and ciprofloxacin on the marine diatom *P. tricornutum*. The findings allowed an evaluation of physiological and genotoxic responses to distinct contaminants.

The contaminants elicited various response patterns. Cadmium initially induced photosynthetic stress and subsequent recovery in all contaminated treatments. In addition, cell density was significantly higher in EC50 after 96 hours, indicating a possible hormetic response. While DNA damage increased with concentration, the impact was not statistically significant, which may be because of short exposure duration or high repair efficiency. Conversely, ciprofloxacin didn't play a role in PSII efficiency in the concentrations tested. Cell density exhibited significant decreases in EC20 and EC50 relative to the control after 96 hours. DNA damage at higher concentrations was severe, being 100% at EC50, although not significantly different when compared with the control. Remarkably, EC10 presented significantly lower genotoxicity compared to the other groups, suggesting a biphasic response.

The investigation validates the susceptibility of *P. tricornutum* to environmentally relevant concentrations of metals and pharmaceuticals and thereby substantiates its application as a test organism in marine ecotoxicology. The integration of physiological and genotoxic endpoints offers further insight into the impact of contaminants, and DNA damage may be regarded as an early sign of cellular stress.

The results of this study enhance the knowledge on the effects of emerging contaminants on marine primary producers and yield relevant data for environmental risk assessment. The methodological protocol validated in this study can be employed to evaluate the effect of various contaminants and their mixtures on marine diatoms, thus aiding in the implementation of efficient biomonitoring programs for marine ecosystem protection. Future directions should concentrate in the development of molecular biomarkers to strengthen the capacity to predict and monitor effects of chemical contamination on marine ecosystems.

6. Bibliographic references

Amin, S. A., Parker, M. S., & Armbrust, E. V. (2012). Interactions between diatoms and bacteria. *Microbiology and Molecular Biology Reviews : MMBR*, *76*(3), 667–684. https://doi.org/10.1128/MMBR.00007-12

Annunziata, R., Balestra, C., Marotta, P., Ruggiero, A., Manfellotto, F., Benvenuto, G., Biffali, E., & Ferrante, M. I. (2021). An optimised method for

intact nuclei isolation from diatoms. *Scientific Reports*, *11*(1), 1681. https://doi.org/10.1038/s41598-021-81238-z

Aristilde, L., Melis, A., & Sposito, G. (2010). Inhibition of Photosynthesis by a Fluoroquinolone Antibiotic. *Environmental Science & Technology*, *44*(4), 1444–1450. https://doi.org/10.1021/es902665n

Baker, N. (2008). Chlorophyll Fluorescence: A Probe of Photosynthesis In Vivo. *Annual Review of Plant Biology*, *59*, 89–113. https://doi.org/10.1146/annurev.arplant.59.032607.092759

Bhatt, S., & Chatterjee, S. (2022). Fluoroquinolone antibiotics: Occurrence, mode of action, resistance, environmental detection, and remediation – A comprehensive review. *Environmental Pollution*, *315*, 120440. https://doi.org/https://doi.org/10.1016/j.envpol.2022.120440

Borowitzka, M. A., & Volcani, B. E. (1978). THE POLYMORPHIC DIATOM PHAEODACTYLUM TRICORNUTUM: ULTRASTRUCTURE OF ITS MORPHOTYPES. *Journal of Phycology*, *14*(1), 10–21. https://doi.org/https://doi.org/10.1111/j.1529-8817.1978.tb00625.x

Branco, D., Lima, A., Almeida, S. F. P., & Figueira, E. (2010). Sensitivity of biochemical markers to evaluate cadmium stress in the freshwater diatom Nitzschia palea (Kützing) W. Smith. *Aquatic Toxicology*, *99*(2), 109–117. https://doi.org/https://doi.org/10.1016/j.aquatox.2010.04.010

Brembu, T., Jørstad, M., Winge, P., Valle, K. C., & Bones, A. M. (2011). Genome-Wide Profiling of Responses to Cadmium in the Diatom Phaeodactylum tricornutum. *Environmental Science & Technology*, *45*(18), 7640–7647. https://doi.org/10.1021/es2002259

Buaya, A., Kraberg, A., & Thines, M. (2019). Dual culture of the oomycete Lagenisma coscinodisci Drebes and Coscinodiscus diatoms as a model for plankton/parasite interactions. *Helgoland Marine Research*, *73*(1), 2. https://doi.org/10.1186/s10152-019-0523-0

Celi, C., Fino, D., & Savorani, F. (2022). Phaeodactylum tricornutum as a source of value-added products: A review on recent developments in cultivation and extraction technologies. *Bioresource Technology Reports*, *19*, 101122. https://doi.org/https://doi.org/10.1016/j.biteb.2022.101122

de With, A., & Greulich, K. O. (1995). Wavelength dependence of laser-induced DNA damage in lymphocytes observed by single-cell gel electrophoresis. *Journal of Photochemistry and Photobiology B: Biology*, *30*(1), 71–76. https://doi.org/https://doi.org/10.1016/1011-1344(95)07151-Q

Dhawan, A., Bajpayee, M., & Parmar, D. (2008). Comet assay: a reliable tool for the assessment of DNA damage in different models. *Cell Biol Toxicol*, *25*(1), 5–32.

Fu, W., Shu, Y., Yi, Z., Su, Y., Pan, Y., Zhang, F., & Brynjolfsson, S. (2022). Diatom morphology and adaptation: Current progress and potentials for

sustainable development. *Sustainable Horizons*, *2*, 100015. https://doi.org/https://doi.org/10.1016/j.horiz.2022.100015

Gorbunov, M. Y., & Falkowski, P. G. (2021). Using Chlorophyll Fluorescence to Determine the Fate of Photons Absorbed by Phytoplankton in the World's Oceans. *Ann Rev Mar Sci*, *14*, 213–238. https://doi.org/10.1146/annurev-marine-032621-122346

Hagenbuch, I. M., & Pinckney, J. L. (2012). Toxic effect of the combined antibiotics ciprofloxacin, lincomycin, and tylosin on two species of marine diatoms. *Water Research*, *46*(16), 5028–5036. https://doi.org/https://doi.org/10.1016/j.watres.2012.06.040

Han, T.-W., Tseng, C.-C., Cai, M., Chen, K., Cheng, S.-Y., & Wang, J. (2020). Effects of Cadmium on Bioaccumulation, Bioabsorption, and Photosynthesis in Sarcodia suiae. *Int J Environ Res Public Health*, *17*(4).

Hendey, N. I., Cushing, D. H., & Ripley, G. W. (1954). Electron Microscope Studies Of Diatoms. *Journal of the Royal Microscopical Society*, *74*(1), 22–34. https://doi.org/https://doi.org/10.1111/j.1365-2818.1954.tb01999.x

Hirsch, R., Ternes, T., Haberer, K., & Kratz, K.-L. (1999). Occurrence of antibiotics in the aquatic environment. *Science of The Total Environment*, *225*(1), 109–118. https://doi.org/https://doi.org/10.1016/S0048-9697(98)00337-4

Honeywill, C., Paterson, D., & Hagerthey, S. (2002). Determination of microphytobenthic biomass using pulse-amplitude modulated minimum fluorescence. *European Journal of Phycology*, *37*(4), 485–492. https://doi.org/10.1017/S0967026202003888

Hooper, D. C. (2001). Mechanisms of Action of Antimicrobials: Focus on Fluoroquinolones. *Clinical Infectious Diseases*, *32*(Supplement_1), S9–S15. https://doi.org/10.1086/319370

International Organization for Standardization. (2018). *Water quality — Marine algal growth inhibition test with Skeletonema sp. and Phaeodactylum tricornutum (ISO Standard No. 10253:2024*). https://www.iso.org/standard/85458.html

Kholssi, R., Lougraimzi, H., & Moreno-Garrido, I. (2023). Effects of global environmental change on microalgal photosynthesis, growth and their distribution. *Marine Environmental Research*, *184*, 105877. https://doi.org/https://doi.org/10.1016/j.marenvres.2023.105877

King, W. G., Rodriguez, J. M., & Wai, C. M. (1974). Losses of trace concentrations of cadmium from aqueous solution during storage in glass containers. *Analytical Chemistry*, *46*(6), 771–773. https://doi.org/10.1021/ac60342a024

Massé, D. I., Saady, N. M. C., & Gilbert, Y. (2014). Potential of Biological Processes to Eliminate Antibiotics in Livestock Manure: An Overview.

Animals : An Open Access Journal from MDPI, *4*(2), 146–163. https://doi.org/10.3390/ani4020146

Moejes, F. W., Succurro, A., Popa, O., Maguire, J., & Ebenhöh, O. (2017). Dynamics of the Bacterial Community Associated with Phaeodactylum tricornutum Cultures. *Processes*, *5*(4). https://doi.org/10.3390/pr5040077

Murchie, E. H., & Lawson, T. (2013). Chlorophyll fluorescence analysis: a guide to good practice and understanding some new applications. *Journal of Experimental Botany*, *64*(13), 3983–3998. https://doi.org/10.1093/jxb/ert208

Olive, P. L., & Banáth, J. P. (2006). The comet assay: a method to measure DNA damage in individual cells. *Nat Protoc*, *1*(1), 23–29.

Ostling, O., & Johanson, K. J. (1984). Microelectrophoretic study of radiation-induced DNA damages in individual mammalian cells. *Biochemical and Biophysical Research Communications*, *123*(1), 291–298. https://doi.org/https://doi.org/10.1016/0006-291X(84)90411-X

Pančić, M., Torres, R. R., Almeda, R., & Kiørboe, T. (2019). Silicified cell walls as a defensive trait in diatoms. *Proceedings of the Royal Society B: Biological Sciences*, *286*(1901), 20190184. https://doi.org/10.1098/rspb.2019.0184

Ruangsomboon, S., & Wongrat, L. (2006). Bioaccumulation of cadmium in an experimental aquatic food chain involving phytoplankton (Chlorella vulgaris), zooplankton (Moina macrocopa), and the predatory catfish Clarias macrocephalus×C. gariepinus. *Aquatic Toxicology*, *78*(1), 15–20. https://doi.org/https://doi.org/10.1016/j.aquatox.2006.01.015

Russo, M. T., Rogato, A., Jaubert, M., Karas, B. J., & Falciatore, A. (2023). Phaeodactylum tricornutum: An established model species for diatom molecular research and an emerging chassis for algal synthetic biology. *Journal of Phycology*, *59*(6), 1114–1122. https://doi.org/https://doi.org/10.1111/jpy.13400

Schreiber, U. (2004). Pulse-Amplitude-Modulation (PAM) Fluorometry and Saturation Pulse Method: An Overview. In G. C. Papageorgiou & Govindjee (Eds.), *Chlorophyll a Fluorescence: A Signature of Photosynthesis* (pp. 279–319). Springer Netherlands. https://doi.org/10.1007/978-1-4020-3218-9_11

Smetacek, V. (1999). Diatoms and the Ocean Carbon Cycle. *Protist*, *150*(1), 25–32. https://doi.org/https://doi.org/10.1016/S1434-4610(99)70006-4

Song, Z., Lye, G. J., & Parker, B. M. (2020). Morphological and biochemical changes in Phaeodactylum tricornutum triggered by culture media: Implications for industrial exploitation. *Algal Research*, *47*, 101822. https://doi.org/https://doi.org/10.1016/j.algal.2020.101822

Stock, W., Blommaert, L., Daveloose, I., Vyverman, W., & Sabbe, K. (2019). Assessing the suitability of Imaging-PAM fluorometry for monitoring growth

of benthic diatoms. *Journal of Experimental Marine Biology and Ecology*, *513*, 35–41. https://doi.org/https://doi.org/10.1016/j.jembe.2019.02.003

Świacka, K., Maculewicz, J., Kowalska, D., & Grace, M. R. (2023). Do pharmaceuticals affect microbial communities in aquatic environments? A review. *Frontiers in Environmental Science*, *Volume 10-2022*. https://doi.org/10.3389/fenvs.2022.1093920

Torres, E., Cid, A., Herrero, C., & Abalde, J. (2000). Effect of Cadmium on Growth, ATP Content, Carbon Fixation and Ultrastructure in the Marine Diatom Phaeodactylum tricornutum Bohlin. *Water, Air, and Soil Pollution*, *117*(1), 1–14. https://doi.org/10.1023/A:1005121012697

Tréguer, P., Bowler, C., Moriceau, B., Dutkiewicz, S., Gehlen, M., Aumont, O., Bittner, L., Dugdale, R., Finkel, Z., Iudicone, D., Jahn, O., Guidi, L., Lasbleiz, M., Leblanc, K., Levy, M., & Pondaven, P. (2018). Influence of diatom diversity on the ocean biological carbon pump. *Nature Geoscience*, *11*(1), 27–37. https://doi.org/10.1038/s41561-017-0028-x